Traffic 2008; **9:** 1878–1893
Blackwell Munksgaard

doi: 10.1111/j.1600-0854.2008.00806.x

Chemical and Biological Folding Contribute to Temperature-Sensitive ΔF508 CFTR Trafficking

Xiaodong Wang[1,2,*], Atanas V. Koulov[3], Wendy A. Kellner[3], John R. Riordan[4] and William E. Balch[1,3,5,*]

[1]Department of Cell Biology, The Scripps Research Institute, 10550 North Torrey Pines Road, La Jolla, CA 92037, USA
[2]Department of Physiology and Pharmacology, The University of Toledo College of Medicine, 3000 Arlington Avenue, Toledo, OH 43614, USA
[3]Department of Chemical Physiology, The Scripps Research Institute, 10550 North Torrey Pines Road, La Jolla, CA 92037, USA
[4]Department of Biochemistry and Biophysics, 5011 Thurston-Bowles Building, University of North Carolina, Chapel Hill, NC 27510, USA
[5]The Institute for Childhood and Neglected Disease, 10550 North Torrey Pines Road, La Jolla, CA 92037, USA
**Corresponding authors: William E. Balch, webalch@scripps.edu and Xiaodong Wang, xiaodong.wang@utoledo.edu*

Received 28 June 2008, revised and accepted for publication 28 July 2008, uncorrected manuscript published online 30 July 2008, published online 28 August 2008

Proteostasis (Balch WE, Morimoto RI, Dillin A, Kelly JW. Adapting proteostasis for disease intervention. Science 2008;319:916–919) refers to the biology that maintains the proteome in health and disease. Proteostasis is challenged by the most common mutant in cystic fibrosis, ΔF508, a chloride channel [the cystic fibrosis transmembrane conductance regulator (CFTR)] that exhibits a temperature-sensitive phenotype for coupling to the coatomer complex II (COPII) transport machine for exit from the endoplasmic reticulum. Whether rescue of export of ΔF508 CFTR at reduced temperature simply reflects energetic stabilization of the chemical fold defined by its primary sequence or requires a unique proteostasis environment is unknown. We now show that reduced temperature (30°C) export of ΔF508 does not occur in some cell types, despite efficient export of wild-type CFTR. We find that ΔF508 export requires a local biological folding environment that is sensitive to heat/stress-inducible factors found in some cell types, suggesting that the energetic stabilization by reduced temperature is necessary, but not sufficient, for export of ΔF508. Thus, the cell may require a proteostasis environment that is in part distinct from the wild-type pathway to restore ΔF508 coupling to COPII. These results are discussed in the context of the energetics of the protein fold and the potential application of small molecules to achieve a proteostasis environment favoring export of a functional form of ΔF508.

Key words: ΔF508, celastrol, CFTR, chemical biology, chloride conductance, cystic fibrosis, endoplasmic reticulum, folding, Golgi, membrane traffic, protein homeostasis, proteostasis, temperature sensitive

Cystic fibrosis (CF) is one of the most common lethal inherited disorders among Caucasians with an incidence of 1 in 2500 live births. The disease is caused by mutations within the gene encoding a cell surface cyclic AMP-dependent chloride channel, the cystic fibrosis transmembrane conductance regulator (CFTR) (1). CFTR is a multimembrane-spanning protein that contains functionally important cytoplasmic domains including the N- and C-termini and the nucleotide-binding domain (NBD) 1, regulatory (R) domain and NBD2 that together regulate channel function and trafficking (2,3). Folding of newly synthesized full-length CFTR *in vivo* requires ~5–10 min, emphasizing the importance of chaperone-mediated folding pathways in coordinating both intradomain and interdomain interactions (4–13).

The most common mutation in CFTR, present in 90% of CF patients, is the deletion of phenylalanine 508 (ΔF508) in the cytosolic NBD1 that triggers misfolding and degradation, leading to the loss-of-function disease. A number of studies from analysis of the folding of recombinant NBD1 *in vitro* have demonstrated that the Phe508 deletion affects the folding kinetics of NBD1 but not the thermodynamic stability of the folded mutant protein when compared with wild-type NBD1 (14–16). Stabilizing the fold with second-site suppressor mutations can eliminate instability (17–19). These *cis*-acting suppressors implicate kinetic instability of the misfolded NBD1 as an early event in the biological folding pathway of CFTR.

The contribution of protein homeostasis or proteostasis programs, that is, the biology that maintains and protects the cellular proteome (20) and that directs CFTR folding (13), remains a major challenge for the field to understand. Patients homozygous for the Phe508 deletion have severe disease. While retaining some channel activity, the ΔF508 CFTR folding defect largely prevents the protein from exiting the endoplasmic reticulum (ER) (2,21,22). As a result, ΔF508 CFTR is principally degraded by ER-associated degradation (ERAD) pathways (23,24). The absence of CFTR on the plasma membrane in a variety of tissues (e.g. lung, pancreas and intestine) results in an imbalance of Na^+, Cl^- and HCO_3^-, leading to a loss of hydration of the extracellular surface. In the case of lung tissue, defective muciliary clearance leads to lung disease, the major cause of premature death (25–29). While a number

of genetic modifiers affect the clinical presentation of CF, they are largely involved in downstream events affecting the severity of disease independent of the initial folding/trafficking pathways (30–32). Thus, the potential importance of factors that affect ΔF508 folding and trafficking and/or the cellular/tissue response to the absence of channel activity leading to the observed clinical phenotype remains to be elucidated (13,33–36).

Export from the ER is dependent on the kinetic and thermodynamic stability of the nascent polypeptide (20,37–39). In this study, ER-associated protein folding (ERAF) and degradation (ERAD) pathways define metabolic pathway(s) that utilizes a variety of general and specialized chaperones comprising the local chaperone environment that are present in either the lumen of the ER or at the cytosolic face to facilitate the folding and stability of the nascent polypeptide (20). Exit from the ER is orchestrated by the COPII vesicle budding machinery that includes the Sar1 guanosine triphosphatase and the coat components Sec23-24 and Sec13-31 (40,41). Sec23-24 functions as a 'selector' that recognizes cargo for export, whereas Sec13-31 functions as a self-assembling 'collector' that concentrates cargo bound to the Sec23-24 adaptor complex to generate transport vesicles that bud from the ER (42). Work by our group and others has shown that selection for export by the Sec24 COPII component involves recognition of a conserved di-acidic exit code found in the cytosolic tail of a number of transmembrane proteins and in the NBD1 domain of CFTR (43–45).

Export of ΔF508 CFTR is temperature sensitive (43,46). At reduced temperature (27–32°C), ΔF508 CFTR can exit the ER, acquire the Golgi-specific *N*-linked glycan modifications and can function as a channel on the cell surface. Curiously, the efficiency of export at reduced temperature, like export at 37°C, appears to be variable among different cell types and is the matter of some debate [(47) and references therein], raising the possibility that a specific chaperone environment (13) and/or other factors mediate export at reduced temperature. Moreover, the restoration of channel conductance following export at reduced temperature appears to be only partial, and its half-life on the cell surface is markedly reduced following transfer of cells back to 37°C where ΔF508 CFTR can be rapidly targeted to the lysosome for degradation, likely through ubiquitin-dependent mechanisms (6,7,21,48–50). Thus, reduced temperature, while supportive of export of ΔF508, does not appear to convey a normal fold trafficking or processing pattern that is fully functional at physiological temperatures.

Previous studies have implicated a role for both the Hsc–Hsp70 and the Hsp90 families of chaperones as well as other components in folding, degradation and export of wild-type and ΔF508 CFTR from the ER at physiological temperature (13,24,51–66). In contrast, the mechanism(s) by which reduced temperature functions to permit ER export of ΔF508 CFTR is largely unknown. One view is that reduced temperature simply conveys kinetic and/or thermodynamic stability to the ΔF508 CFTR chemical folding pathway, a pathway defined by the mutated polypeptide chain sequence (38,67), and that this pathway utilizes the same components as wild-type CFTR. This interpretation is consistent with biochemical studies *in vitro* where the isolated ΔF508 NBD1 domain in solution is kinetically destabilized relative to the wild-type fold (16,17,68). Furthermore, a defect in the chemical fold is supported by the observation that high concentrations of organic solvents such as glycerol that purportedly function only as 'chemical chaperones' by stabilizing the protein fold promote ΔF508 CFTR export *in vivo* at physiological temperatures (15,69–72).

However, a second view is that the variability in export between cell types at reduced temperature involves a biological component(s) to promote the reduced temperature fold. Whether these components are the same or different from those required to fold wild-type CFTR at physiological temperature is unknown. Thus, an alternative, but not mutually exclusive interpretation, is that a different chaperone activity(s) or balance of activities facilitates reduced temperature folding of ΔF508 CFTR when compared with the requirements for wild-type CFTR. If an energetic transition reflecting the change in chemical stability conferred by reduced temperature is the sole mechanism underlying the temperature-dependent export of ΔF508 CFTR from the ER, a specific prediction is that export of ΔF508 CFTR should largely reflect what is seen for wild-type CFTR in the same cell type, albeit with reduced kinetics. In contrast, a chaperone-dependent, perhaps, partially distinct folding pathway model would predict that the temperature-dependent export of ΔF508 CFTR is cell type dependent and does not necessarily correlate with the ability of the cell to export wild-type CFTR, reflecting differences in the local cellular pool(s) of chaperones and their regulators that are available at a particular temperature for export (13,33). This issue has not been explored in any systematic fashion.

To investigate the role of the cellular folding machinery on ΔF508 CFTR export at reduced temperature, we have systematically examined the trafficking of CFTR in two cell lines, human embryonic kidney (HEK) 293 and baby hamster kidney (BHK), each stably expressing either wild-type or ΔF508 CFTR. While both BHK and HEK293 cell lines expressing wild-type CFTR efficiently transport the protein to the cell surface at physiological and reduced temperature, those expressing ΔF508 CFTR display strikingly different phenotypes. In HEK293 cells expressing ΔF508 CFTR (referred to as HEK-ΔF), ΔF508 CFTR efficiently exits the ER at reduced temperature. In contrast, a BHK strain stably expressing ΔF508 CFTR (BHK-ΔF) exported ΔF508 CFTR very poorly at reduced temperature. Mild heat-stress (40°C for 3 h) or acute heat shock (42°C for 30 min) markedly enhanced stability for export of ΔF508 CFTR from the ER in HEK-ΔF cells. However, similar conditions had no effect on export of ΔF508 in

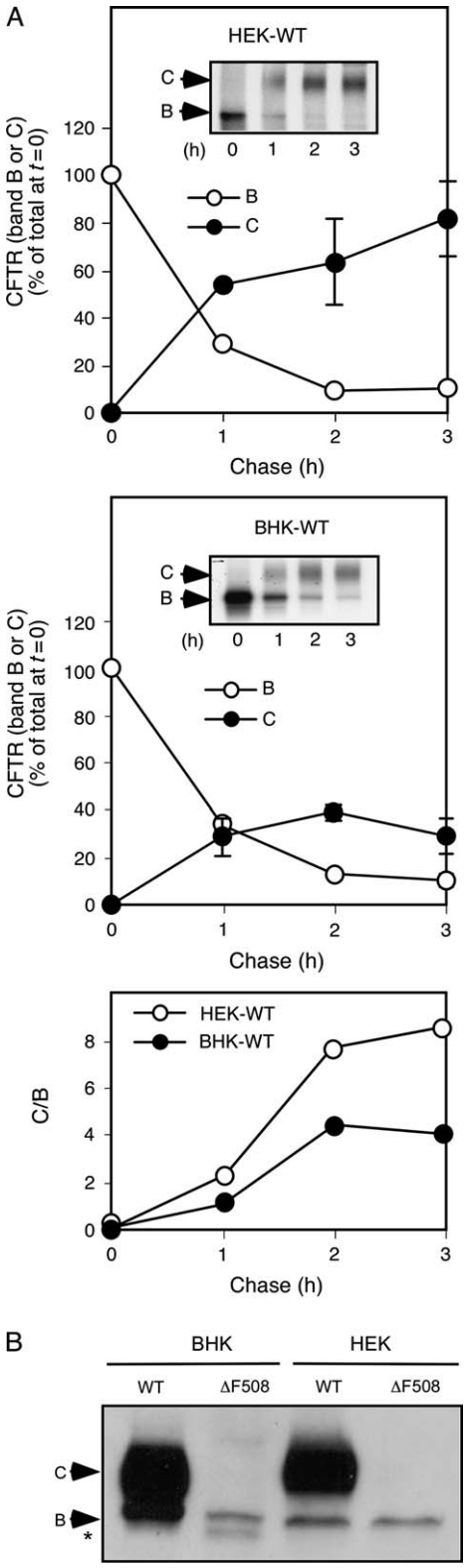

Figure 1: Export of CFTR in BHK and HEK stable cell lines. A) Transport of wild-type CFTR in BHK and HEK293 cells stably expressing the protein at 37°C were performed and analyzed using a pulse–chase protocol as described in the *Materials and Methods*. The percent of CFTR in bands B or C relative to the total observed at time 0 h was determined at the indicated time-points. Experiments were performed in duplicate, and the means and the standard errors of the mean are shown. B) BHK and HEK293 cells stably expressing wild-type or ΔF508 CFTR (BHK-ΔF and HEK-ΔF, respectively) were incubated at 37°C. Cell lysates were separated by SDS–PAGE and immunoblotted with the anti-CFTR monoclonal antibody M3A7. Given that the BHK cell lines express higher levels of CFTR relative to the HEK293 cell lines, BHK lysates were generally loaded at 25–30% total protein relative to that used for HEK293 lysates, with sodium butyrate-induced BHK lysates loaded at 10–15% of that of HEK293 lysates (Figure 2B). Asterisk indicates an ER form that results from translation from a downstream start codon (103).

the BHK-ΔF cell line. Thus, export at reduced temperature appears to be dependent on folding factors that are compatible with the energetics of ΔF508 chain that are available in the HEK293 cells but not in our BHK cell line strain. Such factors may contribute to the variability in cell surface expression of ΔF508 CFTR observed in different cell lines at physiological temperatures and reduced temperatures and have an important impact on our thinking about mechanisms of rescue of ΔF508 folding intermediates in clinical disease.

Results

Transport of wild-type CFTR in HEK293 and BHK cells

We first examined the transport of wild-type CFTR in BHK and HEK293 stable cell lines using a pulse–chase protocol at 37°C. CFTR contains two high-mannose *N*-linked oligosaccharides that are acquired during cotranslational insertion into the ER membrane bilayer (Figure 1, band B) that are processed to the mature form (Figure 1, band C) containing complex sugars during transport through the Golgi to the cell surface (73). As shown in Figure 1A (top panel), HEK293 cells export wild-type CFTR slightly more efficiently (average value of initial total labeled CFTR found in band C is ∼60% at 2 h) when compared with BHK cells (Figure 1A, middle panel) (average value of initial total labeled CFTR found in band C is ∼40% at 2 h), with a proportionately larger pool of the pulse-labeled wild-type CFTR subject to degradation in BHK cells. Despite the apparent slower kinetics of transport of the pulse-labeled pool observed in BHK cells [Figure 1A, compare 1-h time-point in HEK293 (upper panel) versus BHK (middle panel)], based on the steady-state distribution of CFTR at 37°C using immunoblotting of cell lysates, wild-type CFTR largely accumulates in the mature cell surface form (band C) in both cell types. In this study, the core-glycosylated ER form of CFTR (band B) accounts for less than 5–10% of the total pool [an approximate relative ratio of 10:1 for band C to band B, using quantitative immunoblotting of gels

exposed in the linear range (see *Materials and Methods*)] (Figure 1B). In contrast, and consistent with its inability to exit the ER at 37°C, at steady state, ΔF508 is principally if not entirely restricted to the band B form at 37°C in both BHK and HEK293 cells, reflecting ERAD and/or rapid turnover at the cell surface of ΔF508 that escapes the ER (Figure 1B). Thus, although the kinetics and efficiency of export and is less in the BHK cell line as shown by the pulse–chase and the ratio of band C over band B (C/B ratio), a measure of efficiency of export of the pulse–chased CFTR from the ER (Figure 1A, lower panel), both BHK and HEK293 contain the necessary folding machinery to export and maintain wild-type CFTR at the cell surface at physiological temperature. These results are similar to those observed for transport of vesicular stomatitis viral glycoprotein (VSV-G), a type 1 transmembrane protein, that is mobilized rapidly to the cell surface in both cell types at 37°C (data not shown), suggesting that the proteostasis machinery in both cell types is capable of folding and trafficking highly divergent wild-type proteins.

Wild-type CFTR is efficiently exported at both 37°C and 30°C in HEK293 and BHK cells

ΔF508 CFTR is a temperature-sensitive variant that is not efficiently exported from the ER at 37°C but has been shown to exit the ER at reduced temperature (27–32°C). To ensure that reduced temperature does not have a special effect on the function of the folding and export machinery directing wild-type CFTR trafficking, we first examined the effects of reduced temperature on the kinetics of export of wild-type CFTR. HEK293 or BHK cells stably expressing wild-type CFTR were pulsed at 37°C and chased at either 37°C or 30°C (Figure 2A). The pulse at 37°C reflects the steady-state translation and folding properties of both wild-type and ΔF508 CFTR under physiological conditions, the critical concern in disease. As expected, while incubation of cells at reduced temperature resulted in efficient recovery of wild type in band C after 3 h in both cell types (Figure 2A), we observed a modest delay in the decrease of band B and a corresponding slower processing of band B to C when compared with the 37°C incubation in both cells (Figure 2A). Overall, these results are consistent with the conclusion that wild-type CFTR folding and export does not benefit from incubation of cells at lower temperatures, undoubtedly reflecting the higher energetic stability of its folding intermediates when compared with the ΔF508 fold (15,16). Thus, both cell lines possess the machinery to readily direct folding, export and processing of wild-type CFTR at 37°C and 30°C.

ΔF508 shows cell-type-specific export at reduced temperature

To analyze the ability of BHK and HEK293 cells to support temperature-dependent export of ΔF508 CFTR, cell lines stably expressing human ΔF508 CFTR (denoted as BHK-ΔF and HEK-ΔF) were incubated at a range of temperatures for 21 h, and the steady-state distribution of CFTR between bands B and C was analyzed by quantitative immunoblotting (Figure 2B, upper panels). ΔF508 CFTR largely remained in the band B form at 37°C in either cell line based on its distribution at steady state (Figure 2B, inset, upper panel, lane d), although we frequently observed a band of intermediate migration between band B and band C (referred to as band I) in the HEK293 cell line at 37°C and the restrictive temperature (Figure 2B, inset, upper panel, top, lanes d and e) (13). Based upon the intermediate migration of band I and its insensitivity to endoglycosidase H (Figure 2B, inset, lower panel), an enzyme that cleaves ER-associated high-mannose, but not mannose-trimmed, *N*-acetylglucosamine modified Golgi-associated *N*-linked oligosaccharides, band I is likely a partially glycosylated form that appears following transit to early (*cis*/*medial*) Golgi compartments prior to further addition of complex sugars. The latter case is supported by our observations that such Golgi processing intermediates are routinely observed for glycoproteins such as VSV-G transiting the exocytic pathway and are delivered efficiently to the cell surface following further processing to complex oligosaccharides containing galactose and sialic acid (74) (see below).

In HEK-ΔF cells, and consistent with previous reports (46), as the incubation temperature decreased from 37°C to 27°C, the level of total band B observed at steady state decreased with the concomitant appearance of band C (Figure 2B, inset, upper panels, top, lanes a–d). While the appearance of band C was evident between 32°C and 27°C, the highest level of band C occurred at 30°C in HEK-ΔF cells, presumably reflecting a balance between the relative rates of translation, ERAF, ERAD, export from the ER and its cell surface stability. Using the total amount of ΔF508 CFTR exported from the ER reflected in bands I + C (which measures both ER-exported ΔF508 CFTR and its steady-state stability in post-ER compartments and the cell surface) and the total amount in the ER reflected in band B (which measures the steady-state contribution of rates of translation, ERAD and ERAF), we can generate a 'trafficking index' (TI) that is quantitatively defined as the ratio (I + C)/B that defines the overall trafficking environment of CFTR at steady state. This value differs from the C/B ratio observed during pulse–chase that only reflects a small fraction (the pulsed material) of the total CFTR pool in the cell. Thus, in immunoblots, the TI is a value that reflects the overall balance between export of CFTR from the ER and its stability at the cell surface relative to the available band B pool under the indicated incubation conditions. TI serves as a useful index for the relative efficiency of all factors that contribute to the overall trafficking and stability of CFTR in the mature Golgi-processed form at steady state in a given cell type.

At 37°C, the TI for wild-type CFTR encompasses a value range of 10–20 in the HEK293 and BHK cell lines (Figure 1B). At 37°C, the TI for ΔF508 in either cell line under the present incubation conditions is 0.1–0.3, a value that is

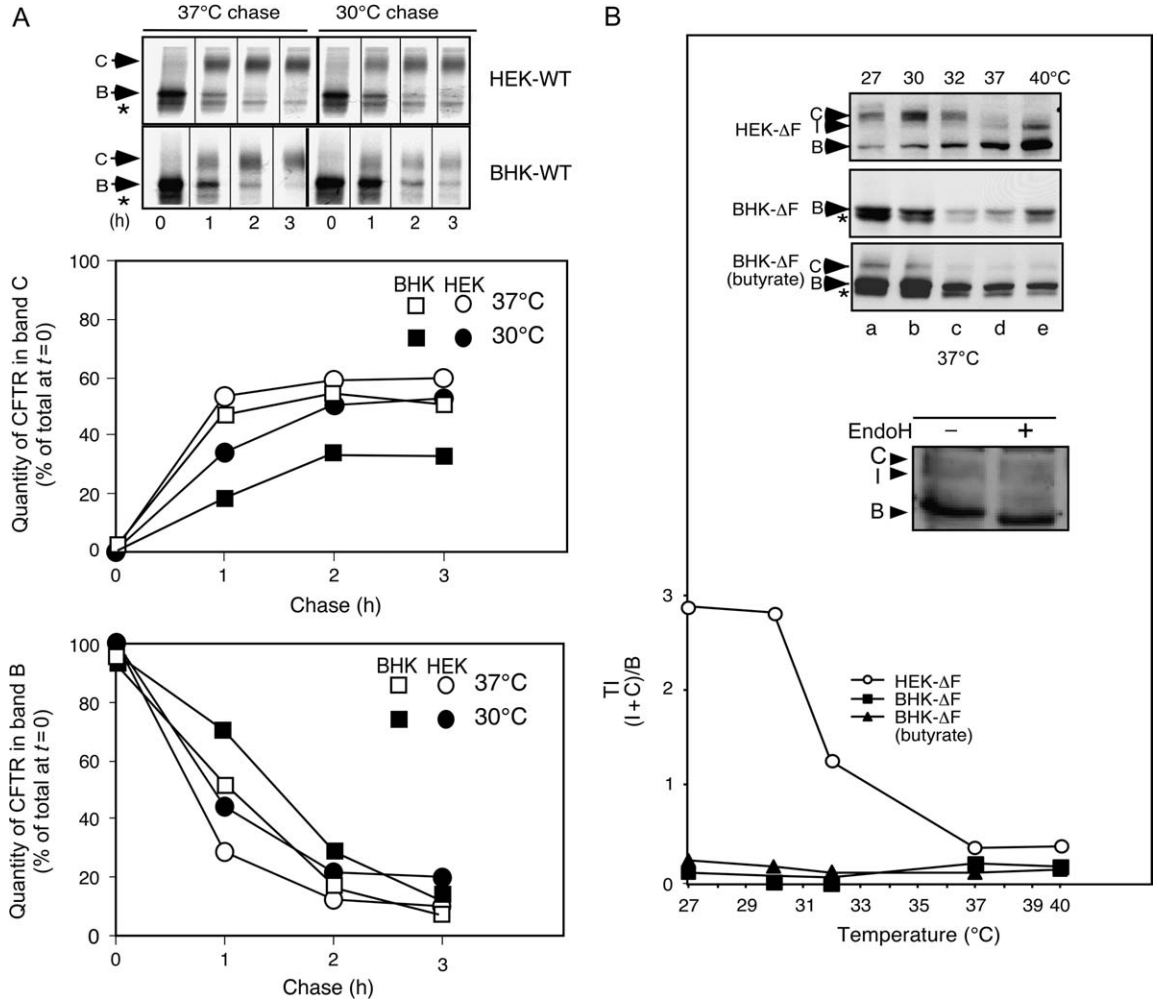

Figure 2: HEK-ΔF but not BHK-ΔF supports the reduced temperature-dependent export of ΔF508 CFTR from the ER. A) HEK cells stably expressing wild-type CFTR were pulsed at 37°C and chased for indicated time at either 37°C or 30°C as described in the *Materials and Methods*. CFTR was recovered by immunoprecipitation, detected by autoradiography and quantified as described in the *Materials and Methods*. The percent of total CFTR in band B or C relative to the total observed at time 0 h was determined at the indicated time-points. B) HEK-ΔF cells were incubated at the indicated temperature for 21 h. BHK-ΔF cells incubated in the absence or presence of sodium butyrate were similarly incubated at the indicated temperature for 21 h. Cells were lysed and equal protein amounts of cell lysate were loaded for each cell type (Figure 1) and separated by SDS–PAGE. CFTR was detected by immunoblotting and quantified as described in the *Materials and Methods*. The (I + C)/B ratio denoted as TI for the distribution of CFTR at steady state was determined as described in the *Results*. Asterisk (see Figure 1 legend).

substantially lower than that of wild-type CFTR. Transfer to 30°C for 21 h results in a ~10-fold increase in the TI of ΔF508 (to ~3) in HEK293 cells (Figure 2B, open circles). Thus, it is apparent that the TI markedly increases with decreasing temperature in HEK293 cells, suggesting an improvement in both folding and export at reduced temperature relative to rates of translation, ERAD and/or cell surface stability. Interestingly, in HEK-ΔF cells, increasing the temperature of incubation from 37°C to 40°C increased the total recovery of both bands B and I (Figure 2B, inset, upper panel, top, lane e) without changing the steady-state value of the TI (Figure 2B, open circles). The increase in band B suggests that additional factors, possibly generated in response to mild heat-stress, may favor the induction of heat shock factors (75) to stabilize the ER-associated but not necessarily post-ER pools (see below).

In contrast to the effects of changing the incubation temperature of HEK-ΔF cells on ΔF508 export and the TI, the BHK-ΔF cell line did not support the low-temperature-dependent export of ΔF508 CFTR from the ER under the current incubation conditions, even though decreased temperature stabilized the steady-state levels of band B when compared with that observed at 37°C (Figure 2B, inset, upper panel, middle lanes a–d). Consistent with these results, the TI largely remained invariant at ~0.1

(Figure 2B, open circles and closed squares). We also observed modest stabilization of band B following incubation under mild heat-stress conditions (40°C), yet no conversion to band I or C (Figure 2B, inset, upper panel, middle, lane e and closed squares). The effects observed were similar when butyrate was added to the culture media to elevate the expression of ΔF508 by 10-fold (Figure 2B, inset, upper panels, bottom), a condition that also yields a TI of ∼0.1 (Figure 2B, triangles), indicating that the absence of rescue does not simply reflect the steady-state pool of CFTR in the ER.

We conclude that both cell lines can stabilize CFTR from degradation in the ER at reduced temperature – evident in the increase in band B. In contrast, HEK-ΔF cells, but not BHK-ΔF cells, have a folding/export machinery that can facilitate an increased recovery of ΔF508 CFTR at the cell surface that is reflected in the increased TI in HEK293-ΔF (∼10-fold), but not in BHK-ΔF, in response to reduced temperature, even though both cell types transport wild-type CFTR within a twofold range at reduced temperature (Figure 2A). Thus, while changes in the chemical fold, that is, the amino acid sequence defining the mutant polypeptide chain, can be stabilized energetically by transfer to reduced temperature, reduced temperature is not sufficient for folding of ΔF508. The mutant appears to require cell-specific factors in addition to those necessary for normal folding and trafficking of wild-type CFTR that are found in HEK293 but not in our strain of BHK.

Reduced temperature kinetically stabilizes band B prior to export

To kinetically characterize the response of ΔF508 CFTR to reduced temperature, we examined the steady-state distribution of ΔF508 CFTR between the ER glycoform (band B) and the post-ER glycoforms (I + C) in each cell line following shift of cells from 37°C to 30°C for increasing time. While we detected a progressive increase in the intensity of band C in HEK-ΔF cells following a brief lag period (Figure 3A,B, approximately eightfold by 21 h), BHK-ΔF cells showed no increase in band C over the same time period of incubation (Figure 3A,B). In HEK-ΔF cells, ΔF508 CFTR transiently appeared in the band I intermediate. In subsequent time-points, band I was reduced and accompanied by appearance of band C (Figure 3A,C). One interpretation is that band I matures to band C as a

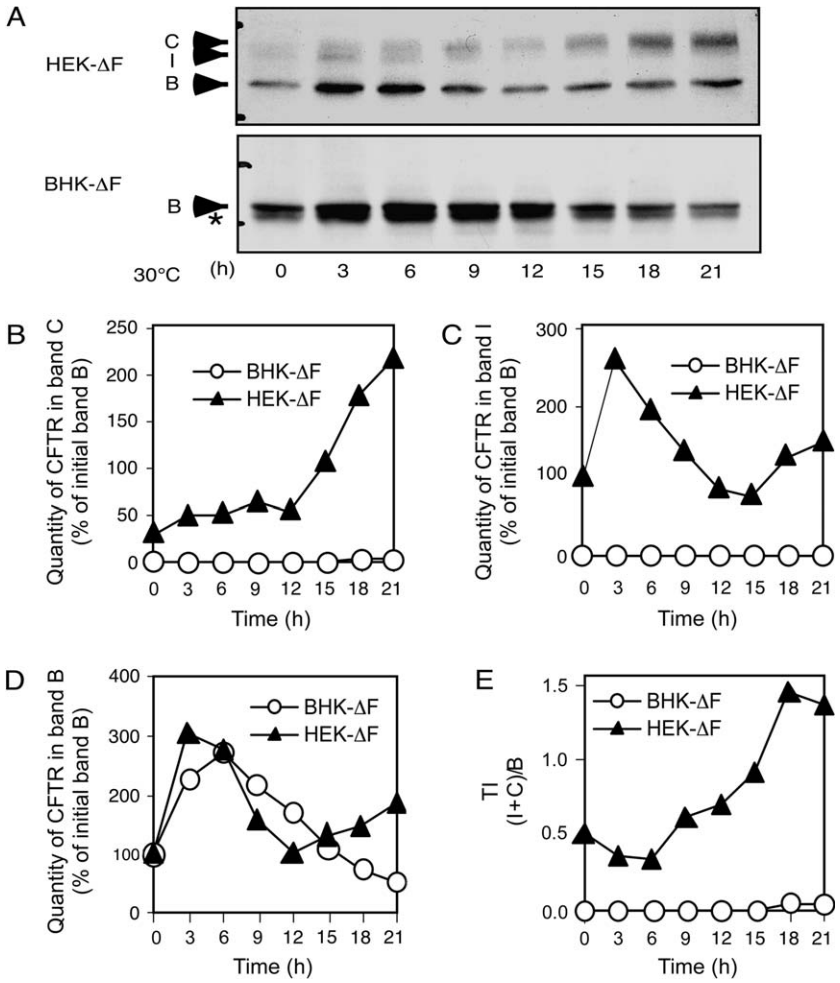

Figure 3: Effect of reduced temperature on ΔF508 transport. A) HEK-ΔF and BHK-ΔF cells were incubated at 30°C for indicated times. Cells were lysed and equal protein amounts of lysates from each cell type were loaded and separated using SDS–PAGE (Figure 1). CFTR was detected by immunoblotting and quantified as described in the *Materials and Methods*. Asterisk (see Figure 1 legend). B–E) Quantification of the levels of B, I or C is expressed as percentage of band B observed at time 0 h (B–D).

consequence of sequential transfer through *cis*, *medial* and *trans* Golgi compartments *en route* to the cell surface, as we have previously demonstrated for VSV-G (74), although we cannot rule out the possibility that band I reflects CFTR retained by the early Golgi or a misfolded form that is degraded as a consequence of recycling to the ER and delivery to ERAD pathways (76,77). In any case, an approximately threefold to fourfold increase in the TI in HEK-ΔF cells (Figure 3E) demonstrates that these cells can export ΔF508 more efficiently than BHK-ΔF by incubation at reduced temperatures for increasing time.

Interestingly, in both cell lines, we first observed significant increase in the levels of band B following shift to 30°C (Figure 3A,D) when compared with the steady-state level observed at 37°C prior to temperature shift. Following the increase, which peaked at 3 h in HEK-ΔF and at 6 h in BHK-ΔF, the steady-state level of band B started to decline, more so in HEK-ΔF cells than in BHK-ΔF cells. In HEK-ΔF cells, these results raise the possibility that at reduced temperature a cellular machinery may initially stabilize nascent ΔF508 CFTR (e.g. band B) in the ER from ERAD relative to the rate of translation. This stabilized conformation could subsequently engage the export machinery, reflected in the transit through the *cis–medial* (band I) (74) and *trans* (band C) Golgi compartments (Figure 3) preceding delivery to the cell surface. In contrast, while BHK-ΔF cells were also able to increase the steady-state level of ΔF508 in the ER, the apparent absence of factor(s) that promotes folding for coupling of the reduced temperature folded band B to the COPII export machinery results in its nearly quantitative degradation. The fact that we observed stabilization of band B in both BHK-ΔF and HEK-ΔF at 30°C, yet no export in BHK-ΔF (Figure 3), demonstrates that a step in common between the two cell types involves partitioning away from the degradation pathway at reduced temperature. However, it is apparent that in BHK cells, the chemical fold induced by temperature shift itself is not sufficient to achieve a conformational change in ΔF508 necessary to engage the COPII machinery. Thus, HEK293 cells contain additional factors to promote folding for protein egress from the ER and stability at the cell surface at reduced temperature.

Heat-stress enhances the export of ΔF508 CFTR at reduced temperature

Numerous studies have focused on the role(s) of chaperones in the delivery of ΔF508 and wild-type CFTR to both ERAD pathways and export (4,10,13,51,53–61,63,78). We noted that mild heat-stress (21 h at 40°C) in HEK293 increased the steady-state level of band B of ΔF508 CFTR and the level of band I proportionally, but not that of band C, relative to that observed at 37°C (Figure 2B, inset, upper panel, top, compare lane d with e). The absence of band C at 40°C suggests that band I is either recycled for ERAD in the ER or processed to band C but is very unstable at the cell surface at this elevated temperature and is rapidly degraded by targeting to lysosome in a fashion that precludes detection at steady state.

To determine if preincubation at 40°C could enhance the level of export of ΔF508 CFTR from the ER following shift to reduced temperature, HEK-ΔF cells were incubated at 40°C overnight (21 h), followed by incubation at 30°C for increasing time as described above. To facilitate comparison, we normalized the steady-state level of ΔF508 CFTR in its ER (band B) and post-ER (band I + C) glycoforms to the level of ΔF508 CFTR in band B at time 0. While incubation at 40°C increased significantly the band B pool in HEK-ΔF cells relative to the no preheat control (Figure 2B, inset, upper panel, top and Figure 4A, $t = 0$), following downshift of these cells to 30°C for 3 h, we observed an additional increase of nascent band B relative to the no preheat control (Figure 4A,B). A similar result was observed for band C (Figure 4A,B), and both continued to increase until ∼9 h (Figure 4A–C). Between 9–15 h, we observed a decrease in both B and C, suggesting loss of the heat-inducible stabilization environment (Figure 4A–C), although typically band I + C began to accumulate again after 15 h. This increase in I + C was correlated with an increase in export efficiency with a TI of ∼2 at 9 h and ∼3 at 21 h (Figure 4A,C,D). We conclude that preheat promotes the transient stabilization and export of ΔF508 CFTR during the subsequent incubation at reduced temperature in a complex fashion, likely reflecting multiple changes in the folding, trafficking and stability environment.

Because BHK-ΔF cells do not support the reduced temperature-dependent export of ΔF508 CFTR (Figures 2 and 3), we examined if a similar approach of mild heat-stress for 21 h at 40°C would rescue the defective export of ΔF508 CFTR in these cells following shift to 30°C. Relative to the no preheat control, neither enhanced stabilization of band B nor appearance of band C was observed (Figure 4E–G).

To further examine the role of mild (40°C) heat-stress in HEK-ΔF, we performed pulse–chase analysis at 30°C following mild treatment of cells for 21 h at 40°C (Figure 5). Consistent with the steady-state results, we observed an approximately twofold enhancement of the initial band B level in heat treated cells versus the no preheat control during the pulse period (Figure 5A, $t = 0$) prior to shift to 30°C. However, following shift to 30°C, we observed a rate of loss of band B that was similar in both the no preheat controls and cell treated at 40°C (Figure 5B,C, open circles), suggesting that the higher level band B observed during the brief pulse at 40°C may represent an increased rate of translation or stabilization. Following temperature shift to 30°C, we observed the expected conversion of labeled ΔF508 CFTR to bands C (Figure 5A and Figure 5B,C, closed circles). The relative export efficiency in heat-treated cells compared with control cells after the 4-h time-point was elevated as reflected in the increase in the ratio of C/B during the pulse–chase. Thus, the increased steady-state level of band C in response to mild heat-stress (Figure 4)

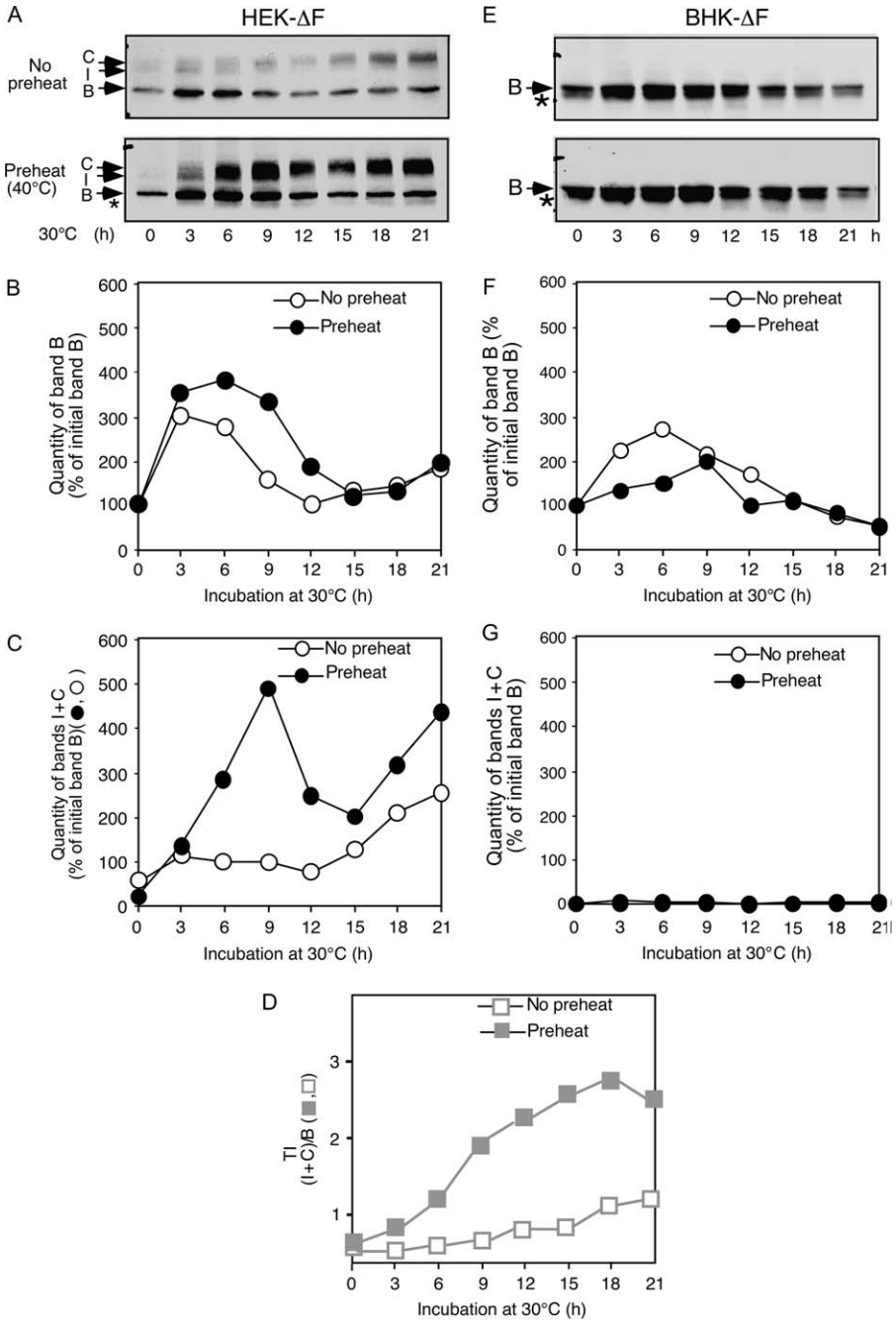

Figure 4: Mild heat-stress promotes export of ΔF508 only in the HEK-ΔF cell line. HEK-ΔF (A–D) and BHK-ΔF (E–G) cell lines were incubated at 30°C for indicated time with or without prior preincubation at 40°C for 21 h. Cells were lysed and equal protein amounts of lysates were loaded (Figure 1) and separated using SDS–PAGE. CFTR was detected by immunoblotting and quantified as described in the *Materials and Methods*. Levels of band B and bands I + C were normalized to the band B density observed at time 0 h. In panel (D), the TI is indicated by the open (no preheat) and closed (preheat) squares. Asterisk (see Figure 1 legend).

appears to reflect a shift toward a pathway in which newly synthesized CFTR favors ER export in HEK293.

A brief exposure to mild heat-stress confers rescue

To determine the minimum time of mild heat treatment (40°C) required to enhance ΔF508 CFTR export, we examined the effect of increasing exposure of cells to 40°C prior to incubation at 30°C or 37°C for 18 h (Figure 6A). Increasing time of exposure to 40°C had a very modest effect on ΔF508 processing upon subsequent incubation of cells at 37°C (Figure 6A,B, upper and middle panels, closed triangles). In contrast, when cells were incubated at 30°C, the effects of mild heat-stress on band B levels and processing to bands I + C were first evident between 0.5- and 3-h preincubation at 40°C (Figure 6A,B, upper and middle panels, closed circles). This increase was blocked by the addition of the transcription inhibitor actinomycin D (Figure 6C), suggesting that inducible factors are likely participating in the high temperature enhancement in ΔF508 CFTR rescue at 30°C. Interestingly, while the recovery of both bands B and C at 30°C were initially improved by preincubation between 0.5 and 3 h at 40°C,

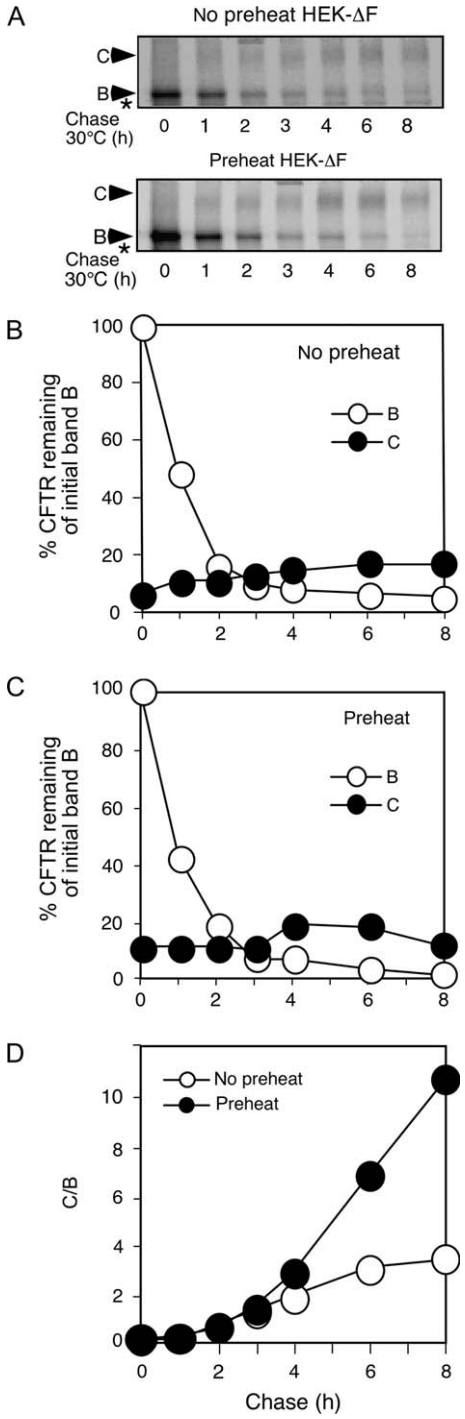

Figure 5: Pulse–chase analysis of the effects of mild heat-stress (40°C) on the export of ΔF508 CFTR at reduced temperature. A) The HEK-ΔF cell line was pulsed at 37°C and chased at 30°C for indicated time with or without prior preincubation at 40°C for 21 h. CFTR was recovered by immunoprecipitation and quantified as described in Figure 1 and the *Materials and Methods*. The two panels were cropped from the same film derived from a single SDS–PAGE. Asterisk (see Figure 1 legend). B and C) Indicated is the percent of CFTR in band B or C relative to the total observed at time 0 h in the no preheat control. D) The C/B ratio is indicated for each time-point in panel (A).

the TI value was not strongly influenced by extending the duration of the mild heat-stress treatment beyond this time-point (Figure 6A,B, lower panel, closed circles). These results suggest that even short exposure to mild heat-stress can augment the efficiency of ER export of ΔF508 CFTR at reduced temperature in HEK-ΔF cells. While we have focused on mild heat-stress (40°C), we have found that acute heat shock (42°C for 30 min) as well as exposure to the heat shock factor 1 (HSF-1)-activating drug celastrol (79,80) yield similar results (data not shown), both largely stabilizing band B prior to appearance of I + C.

Low temperature enhances coupling of ΔF508 CFTR to the COPII machinery in response to changes in cytoplasmic chaperone recruitment

To begin to explore the underlying basis for the temperature-dependent export of ΔF508, we examined its interaction with the Hsp70, Hsp90 and the COPII cargo selection subunit Sec24 (43). For this purpose, HEK-ΔF or BHK-ΔF cells were transferred from 37°C to 30°C and incubated for increasing time. CFTR-containing protein complexes were isolated by coimmunoprecipitation, and components of the CFTR-containing protein complexes were analyzed by immunoblotting. Recovery was normalized to the level of band B in each immunoprecipitate.

In HEK-ΔF cells, Hsp90 showed an initial association that dropped by 60 min of incubation at 30°C (Figure 7A,B, upper panel). In contrast, Hsp70 showed an increase in association with ΔF508 following temperature shift (Figure 7A,B, middle panel) that peaked by 0.5 h and partially declined with increasing time of incubation (Figure 7). Interaction with Sec24 following temperature shift showed a lag period (~1 h) followed by a significant increase at the 3-h time-point, presumably reflecting formation of a transient but larger exportable pool of CFTR (Figure 7A,B, lower panel). Thus, temperature shift appears to result in a temporal response to core inducible folding chaperones (13) that facilitates folding events, leading to stabilization and productive interaction with the COPII machinery in HEK-ΔF cells. In contrast, in the BHK-ΔF cell line, which does not support the export of ΔF508 at reduced temperature, we did not observe a significant change in the recruitment of Hsp70, Hsp90 or Sec24 relative to the total band B present in the immunoprecipitate over the time–course of the experiment (Figure 7). These results underscore a potentially important role for Hsp70/Hsp90 client interactions along with other unknown factors found in HEK293 cells in the conformational maturation of ΔF508 CFTR at reduced temperature for recognition by the COPII machinery.

Discussion

What has not been clearly addressed is the role of chaperone systems in export of ΔF508 from the ER following incubation at reduced temperature. If ΔF508 obtains a more native fold at reduced temperature, then the efficiency of

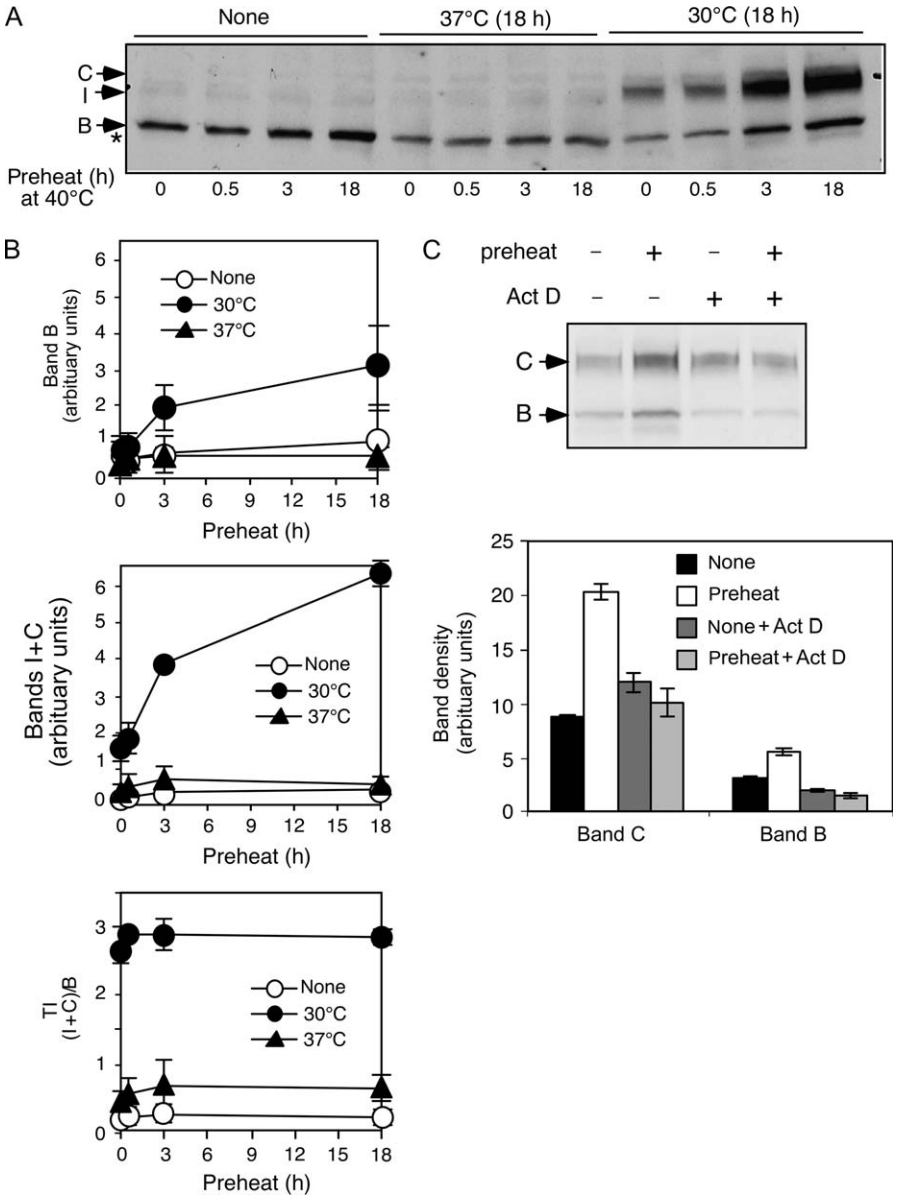

Figure 6: Differential effects of heat-stress on ΔF508 folding and export in the HEK-ΔF cell line. A) HEK-ΔF cells were incubated at 40°C for the indicated time before preparation of cell lysates (time = 0 h), or incubated for an additional 18 h at 37°C or 30°C. Equal protein amounts of cell lysates for each cell time were loaded and separated using SDS–PAGE. CFTR was detected using immunoblotting (representative panel shown) as described in the *Materials and Methods*. Asterisk (see Figure 1 legend). B) The levels of band B (upper panel) and bands I + C (middle panel) are shown for each condition. In the lower panel, the TI is shown. Experiments were conducted in duplicate with the mean and SEM shown. C) HEK-ΔF cells were incubated at 40°C for 3 h (preheat) in the presence or absence of actinomycin D (Act D). Subsequently, the cells were incubated at 30°C for 18 h in the absence of Act D. HEK-ΔF cells without preheat served as controls. Equal protein levels of cell lysates were loaded and separated by SDS–PAGE and the levels of CFTR determined as described in the *Materials and Methods* (representative panel shown). Experiments were conducted in triplicate with the mean and SEM shown in the lower panel.

export should parallel that observed for wild-type CFTR in the same cell line, albeit with reduced kinetics reflecting the decrease in temperature that would presumably stabilize the fold thermodynamically. If, however, reduced temperature represents a unique folding state (either on or off pathway folding intermediates), then, only certain chaperone environments may be capable of supporting folding in a manner that is acceptable for export. Indeed, that is what we found. We suggest that the reduced temperature fold requires processing with a unique balance of components that could differ, at least in part, from the fold generated at physiological temperature. In general, this may be true for a number of temperature-sensitive mutant phenotypes.

Our recent biochemical and biophysical analysis of the export of the 15 kDa secreted protein transthyretin yielded insight into the importance of both kinetic and thermodynamic features of protein folding pathways that contribute to export from the ER (20,37,67). Even energetically destabilized variants were efficiently exported for the ER. These results suggested that export is not necessarily a quality-control-driven pathway, a decision frequently thought to reflect acquisition of an energetically stabilized native fold that prevents targeting to ERAD (81). Rather, this more likely reflects the activity of folding metabolic pathways that is sensitive to a minimum energetic threshold for coupling of cargo to COPII (38). Such pathways are likely unique for each protein fold and are highly adaptable based on the composition of the folding environment (37–39). It is now reasonable to consider the possibility that ΔF508 falls outside an acceptable minimal export energetic threshold (38) at 37°C in most cell types examined. Thus, a limitation

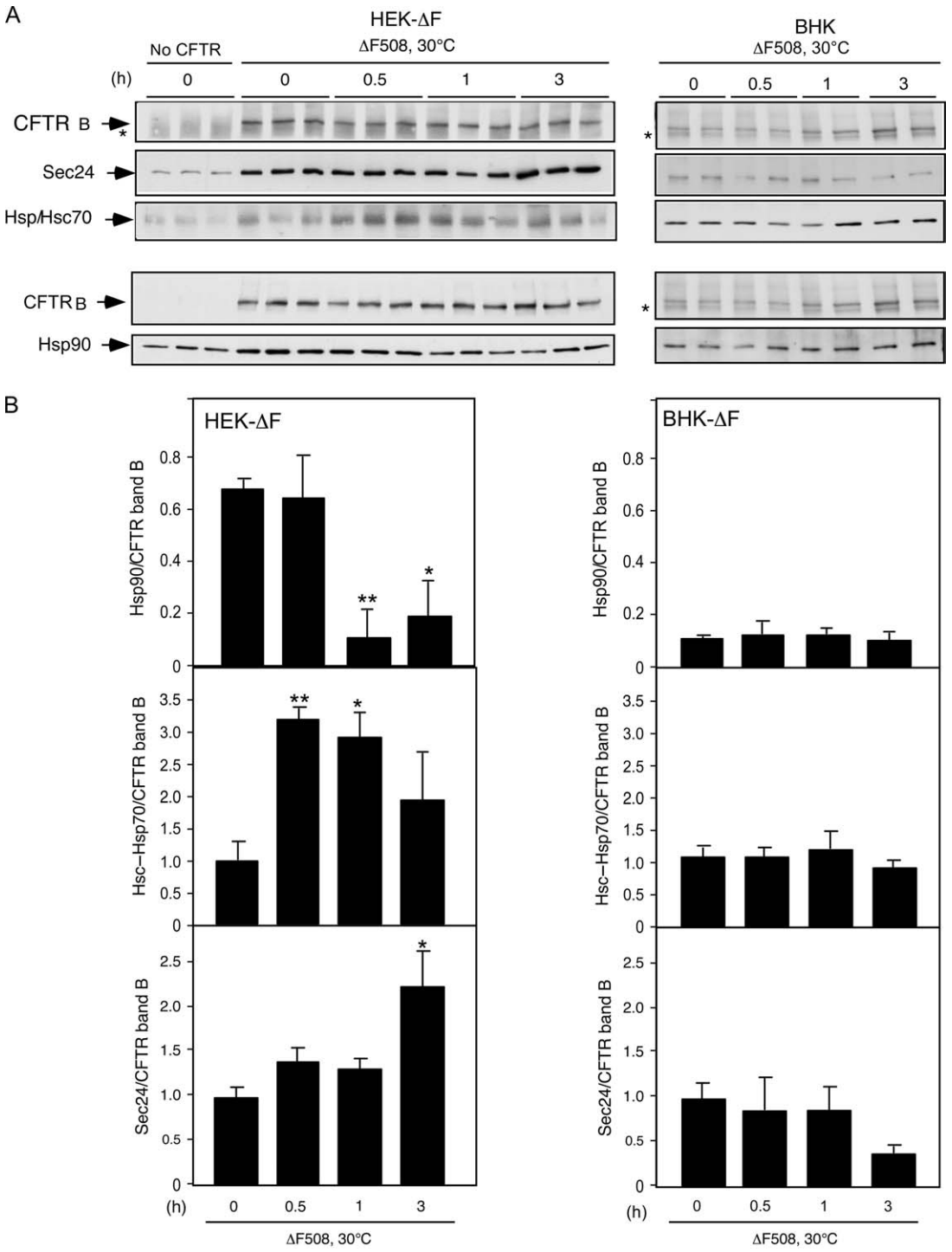

Figure 7: The temperature-dependent export of ΔF508 CFTR in HEK293 cells involves changes in chaperone recruitment followed by increased coupling to Sec24. A) BHK-ΔF or HEK-ΔF cells were incubated at 30°C for the indicated periods of time, and CFTR was recovered by immunoprecipitation as described in the *Materials and Methods*. The immunoprecipitate was separated using SDS–PAGE and analyzed by immunoblotting with the indicated antibodies. HEK293 cells not expressing CFTR served as a negative control. Asterisk (see Figure 1 legend). B) The amount of Hsp90, Hsp70 and Sec24 present in the control (no CFTR) immunoprecipitates was subtracted from the value in each of the corresponding immunoprecipitates and then normalized to the level of CFTR band B recovered at each time-point. The data are expressed as a fractional value relative to the level observed at time 0 h. In HEK-ΔF cells, experiments were conducted in triplicate, and asterisks indicate statistically significant difference between the specific time-point and the zero time-point using the unpaired two-tailed *t*-test analysis (*$p < 0.05$ and **$p < 0.01$). The mean and SEM are shown for duplicate samples with BHK-ΔF cells.

in the kinetics of CFTR folding imposed by the Phe508 deletion emphasizes the possibility that the difference between the export of wild-type and ΔF508 CFTR largely reflects a difference in an energetically prohibitive intermediate folding step within this metabolic pathway dictated by the capacity of the local chaperone biology, that is, the proteostasis environment (20), to adequately support processing of CFTR through the folding pathway (20,38, 39,67). This may reflect the absence of Phe508 in a critical hinge region connecting the NBD1 region to cytoplasmic loop 4 (82), disrupting sequential folding kinetics. The fact that export of ΔF508 and wild-type CFTR may require specialized chaperones found in some mammalian cell lines (e.g. HEK293) but not others (e.g. our BHK-ΔF) helps us to understand why the yeast *Saccharomyces cerevisiae* is unable to support the export of even wild-type CFTR, given its high evolutionary divergence-encompassing significant changes in protein folding and trafficking metabolic pathways that have evolved to handle a different spectrum of cargo folds and their associated energetics (55,57,83). Because yeast ERAD pathways efficiently recognize CFTR and other proteins for degradation (65), we suggest that the unfolded state harbors a more 'ancient' and conserved energetic feature that targets CFTR efficiently to the degradative branch of these pathways. The requirement for a specialized folding machinery is consistent with the highly variable rates of transport of wild-type CFTR and processing of ΔF508 to band C at both reduced temperature and 37°C in different cell lines [(47) and references therein]. This poses a challenge to the CF field in clearly defining the relevant folding and trafficking components responsible for human disease in the lung and other CFTR-requiring tissue environments (13).

Several lines of evidence now favor the interpretation that the kinetic defect in ΔF508 that is bypassed by incubation at reduced temperature reflects potential folding intermediates in the maturation of NBD1 (16,68) and/or its interdomain interactions (5,12,82,84). We have observed that in the CFTR interactome, ΔF508 is potentially trapped in a chaperone-linked folding intermediate(s) (13). Changing the level of activity of one of the Hsp90 co-chaperones found in the folding interactome, Aha1, promoted stability and export of ΔF508 to the cell surface at physiological temperatures with the partial recovery of chloride channel activity (13). These results are consistent with our interpretation that both the composition and the balance of chaperone components that constitute the chaperome environment in the cell can make an important difference in ΔF508 function (13).

We have used the ratio of (I + C)/B as a TI to reflect the overall balance of competing pathways that maintain CFTR in a functional state at the cell surface at steady state. It provides a general measure for comparison of different folding (13), stability and trafficking environments that collectively contribute to this state. While the ratio of ΔF508 and wild-type TIs in HEK293 cells incubated at 30°C was ∼0.3 at steady state, the ratio of ΔF508 to wild-type TIs in BHK cells was nearly an order of magnitude smaller (∼0.03), emphasizing a significant difference in the capacity of the two cell types to produce and maintain a potentially functional pool of ΔF508 at the cell surface at reduced temperature. Thus, at 30°C, the match between the energetics of the chemical fold and the capacity of the local biological folding pathway(s) that can link ΔF508 to the export machinery may be critical for a partially folded intermediate to achieve export and remain stable at the cell surface (37). Indeed, a number of observations show that following export at reduced temperature, shift of cells to 37°C yields a channel with altered function that is more rapidly targeted to lysosome than wild-type CFTR (6,18, 48,50). This could reflect the export of a distinct temperature-dependent, partially destabilized folding intermediate that is not necessarily representative of what we need to achieve in rescue of disease in the normal tissue environment.

We have found that in addition to cell type specificity of ΔF508 CFTR export at reduced temperature, heat-stress protocols (either mild or acute) enhanced export in permissive cells (e.g. HEK293) after temperature shift – more so than at physiologic temperature. We observed that mild heat-stress modified the overall balance of ERAD and export to favor export at reduced temperature, resulting in an improved TI. The effects of heat-stress and stress-related pathways on cellular metabolism are well characterized and involve induction of expression of a large number of cytosolic and ER luminal chaperones among many other components (75,85). Moreover, we have found that small molecules such as celastrol (75) that stimulate the heat shock pathway also stabilize CFTR for reduced temperature export (data not shown) (86). This finding is in agreement with previously projected roles of Hsp70 and Hsp90 pathways in CFTR folding (4,13,24). While stress-inducible factors could include specific Hsp70 and Hsp90 isoforms, they also likely include the many specialized components that regulate ER lumenal or cytosolic chaperome or export pathways (13,56,57,61,63,87–89). Thus, it is apparent that a newly synthesized pool of CFTR transferred to an energetically more permissive folding condition (e.g. reduced temperature) can be more effectively targeted for export when given an enhanced folding environment provided by stress-related responses.

To gain insight into the mechanism of rescue, we observed that HEK-ΔF cells incubated at reduced temperature showed transient changes in the association of ΔF508 CFTR with the COPII component Sec24 (43) and that this change was preceded by changes in the interaction of ΔF508 with Hsp70 and Hsp90 (13,59,60,62,87). Whereas Hsp70 association increased upon shift to reduced temperature prior to restoration of its coupling to the COPII machinery, as scored by recognition of Sec24, we observed a gradual decrease in Hsp90 association raising the possibility that a folding intermediate involving these chaperone systems may become resolved in response to

the change in temperature, although the stoichiometry of these interactions remains to be determined. Whether this indicates that Hsp70 must be recruited to initiate new folding events occurring at reduced temperature or that an improper, more stable interaction of ΔF508 with the Hsp90 chaperone system at physiological temperature precludes export from the ER (13) can be resolved at reduced temperature, or both, remains to be determined.

The ability of cell-specific and heat-inducible factors to increase ΔF508 trafficking from the ER at physiological temperatures raises the possibility that, in addition to small molecules referred to as pharmacological chaperones (PCs) that may directly bind and stabilize the CFTR fold (90–98), another class, which we now refer to as proteostasis regulators (PRs) (20), could be used to augment the folding properties of the cellular chaperome pool to promote rescue (13). Intriguingly, effective PRs might be expected to improve the overall cellular folding/stability environment for a particular mutant, perhaps independent of its cellular location. Thus, unlike reduced temperature, PRs could, in principle, not only stabilize the fold for export at physiological temperature but also, in addition, provide a favorable environment for stability at the cell surface, leading to the observed increase in the TI. The fact that we observe clear differences in the response of ΔF508 to reduced temperature in HEK293 and BHK cells, and to stress-related responses, raises the possibility that different mammalian tissues harboring ΔF508 may respond differentially to both PC and PR approaches (20,38). Our results are consistent with the recent observation that mouse and pig ΔF508 are more efficiently processed to C band than human ΔF508 in a primate, human or pig cell line (99). Thus, not only are the effects of the Phe508 deletion on cell surface delivery dependent on the local folding and trafficking environment (shown herein) but also evolutionary divergent polypeptide chain sequences contribute to the energetic profile that is sensitive to a particular folding environment. This is not unlike the ability of different *cis* suppressor mutations to have differential effects on rescue of the human ΔF508 phenotype (18,19). Identification of the components that define the folding network in different cell types that differentially facilitate ER export and stability of wild-type and ΔF508 CFTR will be critical for our understanding of the balance between the energetics of the chemical fold and the role of biological factors and/or genetic modifiers in CF disease that can influence these pathways (13,30).

Materials and Methods

Antibodies and chemicals

The following antibody reagents were used: a monoclonal antibody (M3A7) against an epitope at the C-terminal end of the second-nucleotide-binding domain of human CFTR (100), monoclonal antibodies 3C5 from B. M. Jockusch (University of Cologne, Cologne, Germany) and 3A3 from Affinity BioReagents that recognizes both constitutive and inducible forms of Hsp70 and an anti-Hsp90 polyclonal antibody Hsp90 (H-114) from Santa Cruz Biotechnology, Inc. The antibodies for Hsp70 and Hsp90 recognize both major isoforms of each protein. Anti-Sec24 polyclonal antibodies were raised against a recombinant fusion protein between glutathione S-transferase and human Sec24C. Protein G Sepharose 4 Fast Flow was purchased from Amersham Biosciences Corp. Celastrol was a kind gift provided by Dr Richard I. Morimoto (Northwestern University, Evanston, IL, USA).

Cell lines

BHK cells stably expressing wild-type or ΔF508 CFTR were obtained from Dr John Riordan, University of North Carolina (101), and were maintained in DMEM supplemented with F12, 5% FBS, 100 units/mL each of penicillin and streptomycin and 500 mM methotrexate (Xanodyne Pharmacal, Inc.). HEK293 cells stably expressing wild-type or ΔF508 CFTR were provided by Dr Neil A. Bradbury (University of Pittsburgh School of Medicine, Pittsburgh, PA, USA) and maintained in DMEM, 10% FBS, 100 units/mL each of penicillin and streptomycin and 150 mg/mL hygromycin B (CN Biosciences, Inc.).

Cell lysis and CFTR quantification

Cells were washed twice with ice-cold (PBS) and lysed in 50 mM Tris–HCl (pH 7.4), 150 mM NaCl and 1% Triton-X-100 (v/v), supplemented with complete protease inhibitor cocktail tablets (Roche Diagnostics GmbH) for 30 min on ice. The lysates were cleared by centrifugation at 16 000 × ***g*** for 20 min. The protein concentration of the lysates was determined using the Coomassie Protein Assay Kit (Pierce Biotechnology), and in most of the experiments, equal protein amounts of lysates were loaded and were separated by SDS–PAGE, immunoblotted with the indicated antibodies and visualized by enhanced chemiluminescence. The density of the bands in the linear exposure range was quantified on a Personal Densitometer SI from Amersham Biosciences Corp., using the image processing program ImageJ (National Institutes of Health) or using an Alpha Innotech Fluorochem SP (Alpha Innotech).

Immunoprecipitation

Monoclonal antibody M3A7 was covalently coupled to Protein G Sepharose 4 Fast Flow beads as described (102). Cells were washed twice with cold PBS and were lysed as described above. The lysates were incubated with the M3A7-coated protein G beads overnight at 4°C. The beads were washed with lysis buffer. CFTR and its coimmunoprecipitating proteins were eluted with 50 mM Tris–HCl (pH 6.8) and 1% SDS. The proteins in the eluant were then separated by SDS–PAGE, immunoblotted with specific antibodies and quantified as described above.

Pulse–chase analysis of CFTR

Cells expressing wild-type CFTR were pulse labeled for 30 min with EasyTag L-^{35}S-Methionine (NEN) and chased in the presence of excess cold Met for the indicated periods of time as described in the Results. For ΔF508-expressing cells, pulse labeling was extended to a total of 1 h to bring the signal to detectible level. CFTR was recovered by immunoprecipitation essentially as described above. The radioactivity of CFTR bands were visualized by autoradiography and quantified by using a PhosphorImager SI or a STORM imaging system (Molecular Dynamics).

Acknowledgments

This study was supported by National Institutes of Health grants GM42336 and 33301 (W. E. B.), DK51870 (J. R. R.), HL79442 (John R. Yates), and Cystic Fibrosis Foundation Research Grant WANG06G0 (X. W.). X. W. and A. V. K. were recipients of postdoctoral research fellowships from the Cystic Fibrosis Foundation, TSRI manuscript number 15-607.

References

1. Riordan JR, Rommens JM, Kerem B, Alon N, Rozmahel R, Grzelczak Z, Zielenski J, Lok S, Plavsic N, Chou JL, Drumm ML, Iannuzzi MC,

Collins FS, Tsui LC. Identification of the cystic fibrosis gene: cloning and characterization of complementary DNA. Science 1989;245: 1066–1073.
2. Riordan JR. Assembly of functional CFTR chloride channels. Annu Rev Physiol 2005;67:701–718.
3. Gadsby DC, Vergani P, Csanady L. The ABC protein turned chloride channel whose failure causes cystic fibrosis. Nature 2006;440:477–483.
4. Amaral MD. CFTR and chaperones: processing and degradation. J Mol Neurosci 2004;23:41–48.
5. Du K, Sharma M, Lukacs GL. The DeltaF508 cystic fibrosis mutation impairs domain-domain interactions and arrests post-translational folding of CFTR. Nat Struct Mol Biol 2005;12:17–25.
6. Sharma M, Pampinella F, Nemes C, Benharouga M, So J, Du K, Bache KG, Papsin B, Zerangue N, Stenmark H, Lukacs GL. Misfolding diverts CFTR from recycling to degradation: quality control at early endosomes. J Cell Biol 2004;164:923–933.
7. Sharma M, Benharouga M, Hu W, Lukacs GL. Conformational and temperature-sensitive stability defects of the delta F508 cystic fibrosis transmembrane conductance regulator in post-endoplasmic reticulum compartments. J Biol Chem 2001;276:8942–8950.
8. Lukacs GL, Mohamed A, Kartner N, Chang XB, Riordan JR, Grinstein S. Conformational maturation of CFTR but not its mutant counterpart (delta F508) occurs in the endoplasmic reticulum and requires ATP. EMBO J 1994;13:6076–6086.
9. Carlson EJ, Pitonzo D, Skach WR. p97 functions as an auxiliary factor to facilitate TM domain extraction during CFTR ER-associated degradation. EMBO J 2006;25:4557–4566.
10. Younger JM, Chen L, Ren HY, Rosser MF, Turnbull EL, Fan CY, Patterson C, Cyr DM. Sequential quality-control checkpoints triage misfolded cystic fibrosis transmembrane conductance regulator. Cell 2006;126:571–582.
11. Kleizen B, van Vlijmen T, de Jonge HR, Braakman I. Folding of CFTR is predominantly cotranslational. Mol Cell 2005;20:277–287.
12. Cui L, Aleksandrov L, Chang XB, Hou YX, He L, Hegedus T, Gentzsch M, Aleksandrov A, Balch WE, Riordan JR. Domain interdependence in the biosynthetic assembly of CFTR. J Mol Biol 2007;365:981–994.
13. Wang X, Venable J, Lapointe P, Hutt DM, Koulov A, Coppinger J, Gurkan C, Kellner W, Matteson J, Plutner H, Roirodan JR, Kelly JW, Yates JRI, Balch WE. Hsp90 co-chaperone Aha1 downregulation rescues misfold of CFTR in cystic fibrosis. Cell 2006;127:803–815.
14. Ostedgaard LS, Zeiher B, Welsh MJ. Processing of CFTR bearing the P574H mutation differs from wild-type and deltaF508-CFTR. J Cell Sci 1999;112:2091–2098.
15. Qu BH, Strickland EH, Thomas PJ. Localization and suppression of a kinetic defect in cystic fibrosis transmembrane conductance regulator folding. J Biol Chem 1997;272:15739–15744.
16. Thibodeau PH, Brautigam CA, Machius M, Thomas PJ. Side chain and backbone contributions of Phe508 to CFTR folding. Nat Struct Mol Biol 2005;12:10–16.
17. Lewis HA, Zhao X, Wang C, Sauder JM, Rooney I, Noland BW, Lorimer D, Kearins MC, Conners K, Condon B, Maloney PC, Guggino WB, Hunt JF, Emtage S. Impact of the deltaF508 mutation in first nucleotide-binding domain of human cystic fibrosis transmembrane conductance regulator on domain folding and structure. J Biol Chem 2005;280:1346–1353.
18. Roxo-Rosa M, Xu Z, Schmidt A, Neto M, Cai Z, Soares CM, Sheppard DN, Amaral MD. Revertant mutants G550E and 4RK rescue cystic fibrosis mutants in the first nucleotide-binding domain of CFTR by different mechanisms. Proc Natl Acad Sci U S A 2006;103:17891–17896.
19. Pissarra LS, Farinha CM, Xu Z, Schmidt A, Thibodeau PH, Cai Z, Thomas PJ, Sheppard DN, Amaral MD. Solubilizing mutations used to crystallize one CFTR domain attenuate the trafficking and channel defects caused by the major cystic fibrosis mutation. Chem Biol 2008; 15:62–69.
20. Balch WE, Morimoto RI, Dillin A, Kelly JW. Adapting proteostasis for disease intervention. Science 2008;319:916–919.
21. Guggino WB, Stanton BA. New insights into cystic fibrosis: molecular switches that regulate CFTR. Nat Rev Mol Cell Biol 2006; 7:426–436.
22. Amaral MD. Processing of CFTR: traversing the cellular maze – how much CFTR needs to go through to avoid cystic fibrosis? Pediatr Pulmonol 2005;39:479–491.
23. Gelman MS, Kopito RR. Cystic fibrosis: premature degradation of mutant proteins as a molecular disease mechanism. Methods Mol Biol 2003;232:27–37.
24. Brodsky JL. The protective and destructive roles played by molecular chaperones during ERAD (endoplasmic-reticulum-associated degradation). Biochem J 2007;404:353–363.
25. Boucher RC. New concepts of the pathogenesis of cystic fibrosis lung disease. Eur Respir J 2004;23:146–158.
26. Tarran R, Button B, Boucher RC. Regulation of normal and cystic fibrosis airway surface liquid volume by phasic shear stress. Annu Rev Physiol 2006;68:543–561.
27. Quinton PM. The neglected ion: HCO3. Nat Med 2001;7:292–293.
28. Quinton PM. Too much salt, too little soda: cystic fibrosis. Sheng Li Xue Bao 2007;59:397–415.
29. Wang Y, Soyombo AA, Shcheynikov N, Zeng W, Dorwart M, Marino CR, Thomas PJ, Muallem S. Slc26a6 regulates CFTR activity in vivo to determine pancreatic duct HCO3-secretion: relevance to cystic fibrosis. EMBO J 2006;25:5049–5057.
30. Cutting GR. Modifier genetics: cystic fibrosis. Annu Rev Genomics Hum Genet 2005;6:237–260.
31. Davies J, Alton E, Griesenbach U. Cystic fibrosis modifier genes. J R Soc Med 2005;98(Suppl. 45):47–54.
32. Slieker MG, Sanders EA, Rijkers GT, Ruven HJ, van der Ent CK. Disease modifying genes in cystic fibrosis. J Cyst Fibros 2005; 4(Suppl. 2):7–13.
33. Ollero M, Brouillard F, Edelman A. Cystic fibrosis enters the proteomics scene: new answers to old questions. Proteomics 2006;6: 4084–4099.
34. Pollard HB, Eidelman O, Jozwik C, Huang W, Srivastava M, Ji XD, McGowan B, Norris CF, Todo T, Darling T, Mogayzel PJ, Zeitlin PL, Wright J, Guggino WB, Metcalf E et al. De novo biosynthetic profiling of high abundance proteins in cystic fibrosis lung epithelial cells. Mol Cell Proteomics 2006;5:1628–1637.
35. Singh OV, Pollard HB, Zeitlin PL. Chemical rescue of F508-CFTR mimics genetic repair in cystic fibrosis bronchial epithelial cells. Mol Cell Proteomics 2008;7:1099–1110.
36. Singh OV, Vij N, Mogayzel PJ Jr, Jozwik C, Pollard HB, Zeitlin PL. Pharmacoproteomics of 4-phenylbutyrate-treated IB3-1 cystic fibrosis bronchial epithelial cells. J Proteome Res 2006;5:562–571.
37. Sekijima Y, Wiseman RL, Matteson J, Hammarstrom P, Miller SR, Sawkar AR, Balch WE, Kelly JW. The biological and chemical basis for tissue-selective amyloid disease. Cell 2005;121:73–85.
38. Wiseman L, Powers E, Kelly JW, Balch WE. The adaptability of protein transport through the secretory pathway. Cell 2007;131:809–821.
39. Wiseman RL, Koulov A, Powers E, Kelly JW, Balch WE. Protein energetics in maturation of the early secretory pathway. Curr Opin Cell Biol 2007;19:359–367.
40. Gurkan C, Stagg SM, Lapointe P, Balch WE. The COPII cage: unifying principles of vesicle coat assembly. Nat Rev Mol Cell Biol 2006;7:727–738.
41. Lee MC, Miller EA, Goldberg J, Orci L, Schekman R. Bi-directional protein transport between the ER and Golgi. Annu Rev Cell Dev Biol 2004;20:87–123.

42. Stagg SM, Gurkan C, Fowler DM, LaPointe P, Foss TR, Potter CS, Carragher B, Balch WE. Structure of the Sec13/31 COPII coat cage. Nature 2006;439:234–238.
43. Wang X, Matteson J, An Y, Moyer BD, Yoo JS, Bannykh S, Riordan JR, Balch WE. COPII-dependent export of cystic fibrosis transmembrane conductance regulator (CFTR) from the ER utilizes a di-acidic exit code. J Cell Biol 2004;167:65–74.
44. Nishimura N, Balch WE. A di-acidic signal required for selective export from the endoplasmic reticulum. Science 1997;277:556–558.
45. Nishimura N, Bannykh S, Slabough S, Matteson J, Altschuler Y, Hahn K, Balch WE. A di-acidic (DXE) code directs concentration of cargo during export from the endoplasmic reticulum. J Biol Chem 1999;274: 15937–15946.
46. Denning GM, Anderson MP, Amara JF, Marshall J, Smith AE, Welsh MJ. Processing of mutant cystic fibrosis transmembrane conductance regulator is temperature-sensitive. Nature 1992;358:761–764.
47. Riordan JR. CFTR function and prospects for therapy. Annu Rev Biochem 2008;77:701–726.
48. Gentzsch M, Chang XB, Cui L, Wu Y, Ozols VV, Choudhury A, Pagano RE, Riordan JR. Endocytic trafficking routes of wild type and DeltaF508 cystic fibrosis transmembrane conductance regulator. Mol Biol Cell 2004;15:2684–2696.
49. Heda GD, Tanwani M, Marino CR. The Delta F508 mutation shortens the biochemical half-life of plasma membrane CFTR in polarized epithelial cells. Am J Physiol Cell Physiol 2001;280:C166–C174.
50. Swiatecka-Urban A, Brown A, Moreau-Marquis S, Renuka J, Coutermarsh B, Barnaby R, Karlson KH, Flotte TR, Fukuda M, Langford GM, Stanton BA. The short apical membrane half-life of rescued {Delta} F508-cystic fibrosis transmembrane conductance regulator (CFTR) results from accelerated endocytosis of {Delta}F508-CFTR in polarized human airway epithelial cells. J Biol Chem 2005;280:36762–36772.
51. Zhang H, Schmidt BZ, Sun F, Condliffe SB, Butterworth MB, Youker RT, Brodsky JL, Aridor M, Frizzell RA. Cysteine string protein monitors late steps in cystic fibrosis transmembrane conductance regulator biogenesis. J Biol Chem 2006;281:11312–11321.
52. Farinha CM, Amaral MD. Most F508del-CFTR is targeted to degradation at an early folding checkpoint and independently of calnexin. Mol Cell Biol 2005;25:5242–5252.
53. Arndt V, Daniel C, Nastainczyk W, Alberti S, Hohfeld J. BAG-2 acts as an inhibitor of the chaperone-associated ubiquitin ligase CHIP. Mol Biol Cell 2005;16:5891–5900.
54. Younger JM, Ren HY, Chen L, Fan CY, Fields A, Patterson C, Cyr DM. A foldable CFTR{Delta}F508 biogenic intermediate accumulates upon inhibition of the Hsc70-CHIP E3 ubiquitin ligase. J Cell Biol 2004;167: 1075–1085.
55. Youker RT, Walsh P, Beilharz T, Lithgow T, Brodsky JL. Distinct roles for the Hsp40 and Hsp90 molecular chaperones during cystic fibrosis transmembrane conductance regulator degradation in yeast. Mol Biol Cell 2004;15:4787–4797.
56. Farinha CM, Nogueira P, Mendes F, Penque D, Amaral MD. The human DnaJ homologue (Hdj)-1/heat-shock protein (Hsp) 40 co-chaperone is required for the in vivo stabilization of the cystic fibrosis transmembrane conductance regulator by Hsp70. Biochem J 2002; 366:797–806.
57. Zhang Y, Nijbroek G, Sullivan ML, McCracken AA, Watkins SC, Michaelis S, Brodsky JL. Hsp70 molecular chaperone facilitates endoplasmic reticulum-associated protein degradation of cystic fibrosis transmembrane conductance regulator in yeast. Mol Biol Cell 2001;12:1303–1314.
58. Meacham GC, Patterson C, Zhang W, Younger JM, Cyr DM. The Hsc70 co-chaperone CHIP targets immature CFTR for proteasomal degradation. Nat Cell Biol 2001;3:100–105.
59. Choo-Kang LR, Zeitlin PL. Induction of HSP70 promotes DeltaF508 CFTR trafficking. Am J Physiol Lung Cell Mol Physiol 2001;281:L58–L68.
60. Rubenstein RC, Zeitlin PL. Sodium 4-phenylbutyrate downregulates Hsc70: implications for intracellular trafficking of DeltaF508-CFTR. Am J Physiol Cell Physiol 2000;278:C259–C267.
61. Meacham GC, Lu Z, King S, Sorscher E, Tousson A, Cyr DM. The Hdj-2/Hsc70 chaperone pair facilitates early steps in CFTR biogenesis. EMBO J 1999;18:1492–1505.
62. Jiang C, Fang SL, Xiao YF, O'Connor SP, Nadler SG, Lee DW, Jefferson DM, Kaplan JM, Smith AE, Cheng SH. Partial restoration of cAMP-stimulated CFTR chloride channel activity in DeltaF508 cells by deoxyspergualin. Am J Physiol 1998;275:C171–C178.
63. Loo MA, Jensen TJ, Cui L, Hou Y, Chang XB, Riordan JR. Perturbation of Hsp90 interaction with nascent CFTR prevents its maturation and accelerates its degradation by the proteasome. EMBO J 1998;17: 6879–6887.
64. Fuller W, Cuthbert AW. Post-translational disruption of the delta F508 cystic fibrosis transmembrane conductance regulator (CFTR)-molecular chaperone complex with geldanamycin stabilizes delta F508 CFTR in the rabbit reticulocyte lysate. J Biol Chem 2000;275: 37462–37468.
65. Ahner A, Nakatsukasa K, Zhang H, Frizzell RA, Brodsky JL. Small heat-shock proteins select deltaF508-CFTR for endoplasmic reticulum-associated degradation. Mol Biol Cell 2007;18:806–814.
66. Sun F, Zhang R, Gong X, Geng X, Drain PF, Frizzell RA. Derlin-1 promotes the efficient degradation of the cystic fibrosis transmembrane conductance regulator (CFTR) and CFTR folding mutants. J Biol Chem 2006;281:36856–36863.
67. Kelly JW, Balch WE. The integration of cell and chemical biology in protein folding. Nat Chem Biol 2006;2:224–227.
68. Qu BH, Thomas PJ. Alteration of the cystic fibrosis transmembrane conductance regulator folding pathway. J Biol Chem 1996;271:7261–7264.
69. Brown CR, Hong-Brown LQ, Biwersi J, Verkman AS, Welch WJ. Chemical chaperones correct the mutant phenotype of the delta F508 cystic fibrosis transmembrane conductance regulator protein. Cell Stress Chaperones 1996;1:117–125.
70. Fischer H, Fukuda N, Barbry P, Illek B, Sartori C, Matthay MA. Partial restoration of defective chloride conductance in DeltaF508 CF mice by trimethylamine oxide. Am J Physiol Lung Cell Mol Physiol 2001; 281:L52–L57.
71. Sato S, Ward CL, Krouse ME, Wine JJ, Kopito RR. Glycerol reverses the misfolding phenotype of the most common cystic fibrosis mutation. J Biol Chem 1996;271:635–638.
72. Zhang XM, Wang XT, Yue H, Leung SW, Thibodeau PH, Thomas PJ, Guggino SE. Organic solutes rescue the functional defect in delta F508 cystic fibrosis transmembrane conductance regulator. J Biol Chem 2003;278:51232–51242.
73. Cheng SH, Gregory RJ, Marshall J, Paul S, Souza DW, White GA, O'Riordan CR, Smith AE. Defective intracellular transport and processing of CFTR is the molecular basis of most cystic fibrosis. Cell 1990;63:827–834.
74. Davidson HW, Balch WE. Differential inhibition of multiple vesicular transport steps between the endoplasmic reticulum and trans Golgi network. J Biol Chem 1993;268:4216–4226.
75. Westerheide SD, Morimoto RI. Heat shock response modulators as therapeutic tools for diseases of protein conformation. J Biol Chem 2005;280:33097–33100.
76. Hegedus T, Aleksandrov A, Cui L, Gentzsch M, Chang XB, Riordan JR. F508del CFTR with two altered RXR motifs escapes from ER quality control but its channel activity is thermally sensitive. Biochim Biophys Acta 2006;1758:565–572.

77. Chang XB, Cui L, Hou YX, Jensen TJ, Aleksandrov AA, Mengos A, Riordan JR. Removal of multiple arginine-framed trafficking signals overcomes misprocessing of delta F508 CFTR present in most patients with cystic fibrosis. Mol Cell 1999;4:137–142.
78. Vij N, Fang S, Zeitlin PL. Selective inhibition of endoplasmic reticulum-associated degradation rescues DeltaF508-cystic fibrosis transmembrane regulator and suppresses interleukin-8 levels: therapeutic implications. J Biol Chem 2006;281:17369–17378.
79. Trott A, West JD, Klaic L, Westerheide SD, Silverman RB, Morimoto RI, Morano KA. Activation of heat shock and antioxidant responses by the natural product celastrol: transcriptional signatures of a thiol-targeted molecule. Mol Biol Cell 2008;19:1104–1112.
80. Westerheide SD, Bosman JD, Mbadugha BN, Kawahara TL, Matsumoto G, Kim S, Gu W, Devlin JP, Silverman RB, Morimoto RI. Celastrols as inducers of the heat shock response and cytoprotection. J Biol Chem 2004;279:56053–56060.
81. Ellgaard L, Helenius A. Quality control in the endoplasmic reticulum. Nat Rev Mol Cell Biol 2003;4:181–191.
82. Serohijos AW, Hegedus T, Aleksandrov AA, He L, Cui L, Dokholyan NV, Riordan JR. Phenylalanine-508 mediates a cytoplasmic-membrane domain contact in the CFTR 3D structure crucial to assembly and channel function. Proc Natl Acad Sci U S A 2008;105:3256–3261.
83. Kiser GL, Gentzsch M, Kloser AK, Balzi E, Wolf DH, Goffeau A, Riordan JR. Expression and degradation of the cystic fibrosis transmembrane conductance regulator in Saccharomyces cerevisiae. Arch Biochem Biophys 2001;390:195–205.
84. Choi MY, Partridge AW, Daniels C, Du K, Lukacs GL, Deber CM. Destabilization of the transmembrane domain induces misfolding in a phenotypic mutant of cystic fibrosis transmembrane conductance regulator. J Biol Chem 2005;280:4968–4974.
85. Young JC, Agashe VR, Siegers K, Hartl FU. Pathways of chaperone-mediated protein folding in the cytosol. Nat Rev Mol Cell Biol 2004;5:781–791.
86. Mu T-W, Ong DST, Segatori L, Wang Y-J, Balch WE, Yates JR III, Kelly JW. Proteostasis regulators and pharmacologic chaperones synergize to restore protein homeostasis in loss-of-function diseases. Cell 2008; in press.
87. Yang Y, Janich S, Cohn JA, Wilson JM. The common variant of cystic fibrosis transmembrane conductance regulator is recognized by hsp70 and degraded in a pre-Golgi nonlysosomal compartment. Proc Natl Acad Sci U S A 1993;90:9480–9484.
88. Strickland E, Qu BH, Millen L, Thomas PJ. The molecular chaperone Hsc70 assists the in vitro folding of the N-terminal nucleotide-binding domain of the cystic fibrosis transmembrane conductance regulator. J Biol Chem 1997;272:25421–25424.
89. Meacham GC, Cyr DM. Isolation of CFTR. Chaperone complexes by co-immunoprecipitation. Methods Mol Med 2002;70:245–256.
90. Verkman AS, Lukacs GL, Galietta LJ. CFTR chloride channel drug discovery – inhibitors as antidiarrheals and activators for therapy of cystic fibrosis. Curr Pharm Des 2006;12:2235–2247.
91. Van Goor F, Straley KS, Cao D, Gonzalez J, Hadida S, Hazlewood A, Joubran J, Knapp T, Makings LR, Miller M, Neuberger T, Olson E, Panchenko V, Rader J, Singh A et al. Rescue of DeltaF508-CFTR trafficking and gating in human cystic fibrosis airway primary cultures by small molecules. Am J Physiol Lung Cell Mol Physiol 2006;290:L1117–L1130.
92. Loo TW, Bartlett MC, Clarke DM. Insertion of an arginine residue into the transmembrane segments corrects protein misfolding. J Biol Chem 2006;281:29436–29440.
93. Loo TW, Bartlett MC, Clarke DM. Rescue of DeltaF508 and other misprocessed CFTR mutants by a novel quinazoline compound. Mol Pharm 2005;2:407–413.
94. Loo TW, Bartlett MC, Wang Y, Clarke DM. The chemical chaperone CFcor-325 repairs folding defects in the transmembrane domains of CFTR-processing mutants. Biochem J 2006;395:537–542.
95. Norez C, Antigny F, Becq F, Vandebrouck C. Maintaining low Ca2+ level in the endoplasmic reticulum restores abnormal endogenous F508del-CFTR trafficking in airway epithelial cells. Traffic 2006;7:562–573.
96. Norez C, Noel S, Wilke M, Bijvelds M, Jorna H, Melin P, DeJonge H, Becq F. Rescue of functional delF508-CFTR channels in cystic fibrosis epithelial cells by the alpha-glucosidase inhibitor miglustat. FEBS Lett 2006;580:2081–2086.
97. Lipecka J, Norez C, Bensalem N, Baudouin-Legros M, Planelles G, Becq F, Edelman A, Davezac N. Rescue of DeltaF508-CFTR (cystic fibrosis transmembrane conductance regulator) by curcumin: involvement of the keratin 18 network. J Pharmacol Exp Ther 2006;317:500–505.
98. Dormer RL, Harris CM, Clark Z, Pereira MM, Doull IJ, Norez C, Becq F, McPherson MA. Sildenafil (Viagra) corrects DeltaF508-CFTR location in nasal epithelial cells from patients with cystic fibrosis. Thorax 2005;60:55–59.
99. Ostedgaard LS, Rogers CS, Dong Q, Randak CO, Vermeer DW, Rokhlina T, Karp PH, Welsh MJ. Processing and function of CFTR-DeltaF508 are species-dependent. Proc Natl Acad Sci U S A 2007;104:15370–15375.
100. Kartner N, Augustinas O, Jensen TJ, Naismith AL, Riordan JR. Mislocalization of delta F508 CFTR in cystic fibrosis sweat gland. Nat Genet 1992;1:321–327.
101. Seibert FS, Tabcharani JA, Chang XB, Dulhanty AM, Mathews C, Hanrahan JW, Riordan JR. cAMP-dependent protein kinase-mediated phosphorylation of cystic fibrosis transmembrane conductance regulator residue Ser-753 and its role in channel activation. J Biol Chem 1995;270:2158–2162.
102. Harlow E, Lane D. Antibodies: A Laboratory Manual. Cold Spring Harbor: Cold Spring Harbor Laboratory; 1988.
103. Pind S, Riordan JR, Williams DB. Participation of the endoplasmic reticulum chaperone calnexin (p88, IP90) in the biogenesis of the cystic fibrosis transmembrane conductance regulator. J Biol Chem 1994;269:12784–12788.